This article has been accepted for publication in IEEE Transactions on Power Systems. This is the author's version which has not been fully edited and content may change prior to final publication. Citation information: DOI 10.1109/TPWRS.2022.3216639

A Methodology to Evaluate Reactive Power Reserves Scarcity during the Energy Transition

Elnaz Davoodi, Florin Capitanescu, *Member, IEEE*, Louis Wehenkel

***Abstract*—The lack of reserves for reactive power production and absorption is an envisioned, still basically unexplored, threat to the voltage profile adequacy and thereby secure operation of transmission grids during the energy transition toward renewable-dominated power production. This paper proposes a novel, generic, comprehensive, and realistic methodology to identify when this issue of reactive power reserves (RPRs) scarcity during plausible scenarios of the energy transition would become severe. The computational core of the proposed methodology comprises four different AC security-constrained optimal power flow (SCOPF) problems: one conventional, two tailored ones that assess the RPRs scarcity in production and absorption modes, respectively, and an optimal reactive power dispatch. The methodology is versatile, offering the possibility to assess RPRs in different timescales, ranging from day-ahead short-term operation to years-ahead long-term operation, and considering appropriate renewable energy production forecasts and day-dependent load profiles. The proposed methodology can serve as a decision support tool for the transmission system operator (TSO), allowing to plug and play different plausible energy transition scenarios (e.g., differing in terms of sequence and timing of: phased out power plants as well as location, type, and size of renewable energy sources deployed) and ultimately informing the TSO about the timing where RPRs become insufficient to maintain security. Without loss of generality, the value of the proposed methodology is extensively demonstrated in a 60-bus Nordic32 system, considering 52 $N-1$ line and generator contingencies, while the tractability of AC SCOPF problems is assessed in a 1,203-bus system.**

***Index Terms*—power system operation, reactive power reserves, security-constrained optimal power flow**

NOMENCLATURE

A. Sets

$\mathcal{B}$	Set of buses
$\mathcal{C}$	Set of postulated contingencies
$\mathcal{D}$	Set of buses with loads
$\mathcal{G}$	Set of buses with conventional generation
$\mathcal{L}$	Set of branches (lines and transformers)
$\mathcal{S}$	Set of buses with solar power generation
$\mathcal{W}$	Set of buses with wind power generation

B. Variables

$\alpha_i^{\text{w,s,d}}$	Wind, solar, demand shedding proportion at bus i
e_i^c/f_i^c	Real/imaginary component of the complex voltage at bus i in state c
P_i^c/Q_i^c	Active/reactive power injection at bus i in state c
$P_i^{\text{g},c}/Q_i^{\text{g},c}$	Active/reactive power output of the generator at bus i in state c
$Q_i^{\text{s/w},c}$	Reactive power output of the solar and wind at bus i in state c
$Q_i^{c,\max}$	Maximum reactive power of the generator at bus i in state c
RQ_i^{g}	Reactive power reserve of the generator at bus i
V_i^c	Voltage magnitude at bus i in state c $(\sqrt{(e_i^c)^2+(f_i^c)^2})$

C. Parameters

b_i^{sh}	Susceptance of the shunt capacitor/reactor at bus i
b_{ij}^c/g_{ij}^c	Susceptance/conductance of the branch ij linking buses i and j in state c
c_i	Cost of the active power generation at bus i
ΔP_i^{g}	Active power ramp rate of the generator at bus i
$E_{f,i}^{\max}$	Maximum field (rotor) induced voltage of the generator at bus i
$I_i^{s,\max}$	Maximum stator current of the generator at bus i
$P_i^{\text{d}}/Q_i^{\text{d}}$	Active/reactive power demand at bus i
$P_i^{\text{s/w}}$	Active power output of the solar/wind at bus i
r_{ij}	Ratio of the transformer in branch ij ($r_{ij}=1$ if the branch is a line)
$w^{\text{w/s/d}}$	Wind/solar/demand shedding costs
X_i^g	Synchronous reactance of the generator at bus i
$\bullet^{\max}$	Upper limit on I_{ij}^c, $P_i^{\text{g},c}$, V_i^c and $Q_i^{\text{s/w},c}$
$\bullet^{\min}$	Lower limit on $P_i^{\text{g},c}$, $Q_i^{\text{g},c}$, V_i^c and $Q_i^{\text{s/w},c}$

The authors acknowledge the funding from Luxembourg National Research Fund (FNR) in the framework of the project ML4SCOPF (INTER/FNRS/19/14015062). This work was supported by the Fonds de la Recherche Scientifique - FNRS under grant T.058.20. E. Davoodi and F. Capitanescu are with Luxembourg Institute of Science and Technology (elnaz.davoodi, florin.capitanescu@list.lu) and L. Wehenkel is with the University of Liege, Belgium (l.wehenkel@uliege.be).

I. INTRODUCTION

A. Motivation

DURING the ongoing "energy transition" towards a sustainable, renewable-dominated, electricity supply [1], [2], the secure operation of the transmission grid will be threatened mainly due to the variability and limited dispatchability of *renewable energy sources* (RES) such as wind turbines and solar photovoltaic, which are gradually displacing environmentally unfriendly conventional power plants.

A major envisioned threat to system security during the energy transition, the subject of this paper and yet severely under-addressed, is that the transmission grid may face extreme situations of lack or excess of reactive power [3], [4] and consequently experience under-voltage (or even voltage instability) and over-voltages, respectively. The root cause of

this threat is that RES cannot deliver the same high standard of reactive power as conventional power plants due to the following reasons. As regards the variable RES connected at the transmission level:

- unlike conventional power plants, which were planned at appropriate locations to face predictable operation conditions, RES have been located where the climate conditions are suitable (e.g., off-shore for wind power). Accordingly, as reactive power does not travel far, such RES physical reserve could be only partly useful. Besides, it is not located in a suitable place to support the high load of cities.
- For the same size, the reactive power capability of RES is lower than that of synchronous generators (e.g., wind RES reactive power limits are between -30% and 40% of the maximum active power [5], i.e., significantly lower than for a conventional generator).
- RES based on power electronics are more sensitive than conventional generators and their behavior is less well understood under unusual operating conditions; hence they may unexpectedly disconnect, depriving the system of valuable reserves (see e.g., the recent UK event [6]).

As regards RES connected to distribution systems:

- Although RES are able to provide reactive power support (as per IEEE std 1547-2018 [7], that could be adopted to different extents and various country-specifics by operators), they are still operating at (often unitary) constant power factor, as deployed according to the grid code [5], [8] (e.g., PV panels in low voltage grids). Therefore, their capability remains unexploited because it is financially and logistically prohibitive to send crews to change manually the inverter settings of privately owned PV panels.
- Some RES that may control their reactive power are outside the TSO jurisdiction. Such RES could be either already involved in the optimal management of active distribution networks or part of their physical reserve may be ineffective due to congestion, voltage issues, or loss increase.
- As reactive power has a strong local impact, it is rather ineffective for remote transmission system support due to several stages of transformers (from low to high voltages).

This threat is further exacerbated by unplanned demand versus generation patterns and hence may stress the grid in regions where reactive power support is scarce.

B. Literature review

Evaluating when *reactive power reserves* (RPRs) may become scarce during the energy transition is hence both timely and relevant; it was partly addressed through a crude preliminary approach [4]. RPRs scarcity identification is a first step that will inform the subsequent problem of determining the optimal size and location of RPRs during the energy transition via var planning [9], [10]. These researches have been framed as specific cases of *security constrained optimal power flow* (SCOPF) framework, which targets ensuring $N-1$ security with respect to thermal limits, bus voltage magnitude limits, and sometimes voltage or angle stability (modeled by surrogate constraints).

Before the strong push for sustainable power grids, in the old power system paradigm, there have been substantial efforts to evaluate and manage reactive power in two respects: (i) *the reactive power support* and (ii) *reactive power reserves*.

In the context of reactive power support, Ref. [11] establishes an approach for valuing and compensating dynamic reactive power support services through the new concept of equivalent var value. Ref. [12] addresses the problem of reactive power procurement by an independent system operator in deregulated electricity markets. It concludes that the operator tends to procure reactive power support from those providers who possess high marginal benefit from the service with price bids within acceptable ranges. Ref. [13] proposes a new approach to design reactive power capacity markets where reactive power procurement could be conducted by the system operator under the proposed approach annual auction. Current trends and progress in reactive power procurement have been reviewed in [14] considering different procurement mechanisms and related compensation schemes.

The RPRs provision has been viewed from the load and generation perspectives [15], [16]. From the load' point of view, the emphasis is on the margin to voltage instability. From the generation's perspective, the focus is on the amount of reactive power reserve provided by the generators. Ref. [17] establishes the concept of *effective* RPR of a generator as the largest amount of reserve the generator provides in response to a set of $N-1$ contingencies as long as the system operation is viable.

Based on the aforementioned RPRs' perspectives, Ref. [18] relies on the concept of effective RPRs and evaluates the impact of generators on the maximum permissible loading of buses. This information is especially useful for analyzing the reactive power reserves of the generators when the system faces voltage collapse. To this end, the proposed approach in [19] enhances the post-contingency voltage stability margins of severe contingencies using the existing reactive resources. Ref. [20] proposes a two-step approach to evaluate reactive power reserves with respect to operating constraints and voltage stability for a set of postulated operating scenarios. At first, a SCOPF problem achieves the minimum overall needed RPRs; then, additional RPRs are determined to ensure voltage stability of the scenarios. Following up, Ref. [4] raises awareness about the reactive power reserves scarcity as one move toward renewable-dominated electricity supply and presents a crude first version of a methodology to predict such upcoming issues. Finally, Ref. [21] discusses real-time aspects of RPRs, pointing out that the effective monitoring of var capability and RPR of wind farms is affected by a few factors like wind conditions, external power grid approximation, and internal operation constraints.

C. Contributions of the Work

In response to the challenges and needs identified so far, the *main original contribution* of this paper is a *generic*, *comprehensive* and *realistic* methodology to gauge RPRs scarcity during plausible scenarios of the energy transition, which includes primarily the development of AC SCOPF-based modules to minimize RPRs in *production* and *absorption* modes. In

This article has been accepted for publication in IEEE Transactions on Power Systems. This is the author's version which has not been fully edited and content may change prior to final publication. Citation information: DOI 10.1109/TPWRS.2022.3216639

addition, for comprehensiveness, the methodology adapts and integrates some existing modules such as:

- an enhanced *conventional AC SCOPF* to maintain $N-1$ security, which feeds the two AC SCOPF-based modules minimizing RPRs;
- an AC SCOPF-based tailored reactive power re-dispatch;
- realistic models of reactive power limits of synchronous generators, that depend on the produced active power and terminal voltage as well as include rotor and stator current limits. These models are embedded in all SCOPF modules.
- the *auto regressive integrated moving average* (ARIMA) model [22], to forecast the power production of RES (wind and solar farms) assumed to be deployed in the system during the energy transition scenario, and load profiles depending on the type of day.

The proposed methodology can serve as a decision-making support tool for the TSO to assess RPRs in different time scales, ranging from a day-ahead *short-term* operation to a years-ahead *long-term* operation. It allows to plug and play different plausible energy transition scenarios (e.g., differing in terms of sequence and timing of: phased out power plants, location, type, and size of RES), and ultimately informs the TSO about the timing where RPRs become insufficient to maintain security.

II. The Proposed Methodology

A. Principle, Assumptions and Scope

This section presents the proposed methodology (see Fig. 1) to evaluate RPRs scarcity during postulated energy transition scenarios. The methodology contains two time-frames that will be described in detail hereafter: day-ahead short-term operation (see the inner loop) and years-ahead long-term operation (see the outer loop). Let us stress that the time needed to address at the planning stage the scarcity of RPRs (e.g., to be corrected via var planning through SVCs, shunt compensation, etc.) is significantly shorter than for the scarcity of active power (corrected via generation expansion) or transmission capacity (corrected via network expansion). For example, the former would roughly require much faster assets field deployment, possible even in a range of several months and up to one year, while the two latter would need typically at least 5-10 years before actual deployment. Accordingly, the outer loop assumes a time horizon of up to 5 years ahead. Albeit inspired by Europe, where the energy transition scenarios focus typically on replacing fossil fuel generation with mostly wind and solar RES, *the methodology is generic* and can be applied with minor adaptations to any other specific context including different combinations (types and mix) of electricity production sources (e.g., hydro, nuclear, biomass).

We consider three types of RPRs of a generator classed in decreasing order of their range:

- Physical one (i.e., the difference between the physical limit and the initial reactive power production);
- The *effective* RPR is the largest amount of reserve the generator utilizes in response to a set of $N-1$ contingencies as long as the system operation is viable [17]. For instance, if the voltages drop at alarmingly low values and the system is collapsing, a big chunk of physical RPR may be useless. Accordingly, due to the transmission grid characteristics, reactive power does not travel far, for most generators the effective RPR is lower than the physical one. The effective RPR can be obtained after post-processing the solution of conventional SCOPF as will be explained hereafter.
- The *necessary* RPR is the utilized amount of reserve of the generator that corresponds to the *minimum overall utilized reserve over all generators* such that the system operation

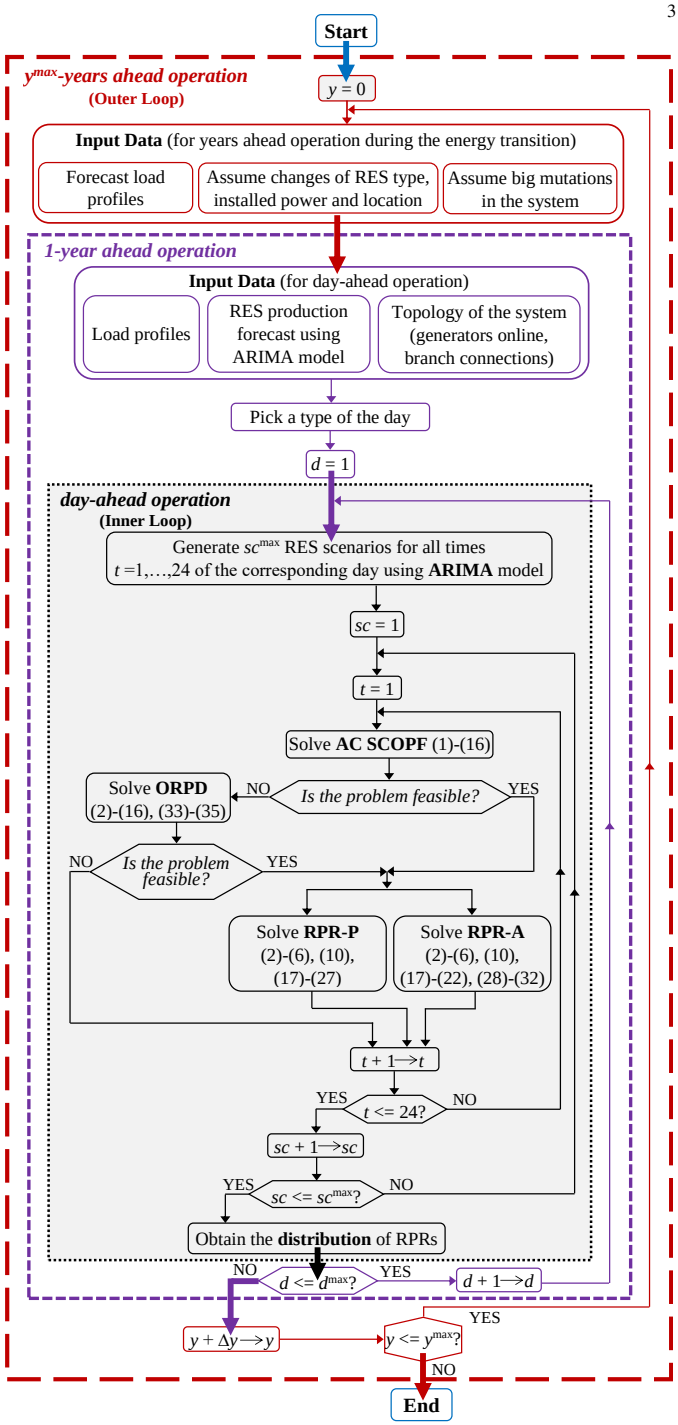

Fig. 1: Flowchart of the proposed methodology.

is viable in response to a set of $N-1$ contingencies. However, the necessary RPR is not necessarily smaller than the effective RPR for each individual generator, see Fig. 3. The effective and necessary RPRs are state independent. The necessary RPR is calculated at the solution of proposed minimizers of RPRs in production and absorption modes described hereafter.

B. The Inner Loop for Short-Term Operation

1) Aim

The goal in day-ahead operation is to evaluate the necessary RPRs for every hour of the next day ($t = 1, \ldots, 24$) and for a number of RES production sampled scenarios ($sc = 1, \ldots, sc^{\max}$), see the inner loop in Fig. 1. These scenarios correspond to forecasted wind and solar RES power production through the next day and are generated using the auto regressive integrated moving average model (ARIMA) [22], [23].

The inner loop contains four distinct computation modules that resort to nonlinear programming formulations:

1) the simulator of operation, via an enhanced "conventional" AC SCOPF computation,
2) the minimizer of overall necessary RPRs in *production* mode (RPR-P),
3) the minimizer of overall necessary RPRs in *absorption* mode (RPR-A)
4) the optimal reactive power dispatch (ORPD) AC SCOPF.

These modules are called for every combination of time step t and RES production scenario sc. Eventually, the analysis of the so-obtained RPRs can reveal instances where the reserves are insufficient, which is valuable information to the TSO.

The mathematical formulations of the four AC SCOPF problems, provided next, rely on voltage rectangular coordinates and adopt the preventive-corrective mode [24].

2) The Conventional Enhanced AC SCOPF

The role of the conventional SCOPF computation is to mimic an operator minimizing the cost of meeting all power system constraints in normal operation and for a set $\mathcal{C}$ of contingencies:

$$\min_{P_i^{\mathrm{g},c}, Q_i^{\mathrm{g},c}, V_i^{g,c}, \alpha_i^{\mathrm{w/s/d}}} \sum_{i\in\mathcal{G}} c_i P_i^{\mathrm{g},0} + w^{\mathrm{d}} \sum_{i\in\mathcal{D}} \alpha_i^{\mathrm{d}} P_i^{\mathrm{d}} + w^{\mathrm{w}} \sum_{i\in\mathcal{W}} \alpha_i^{\mathrm{w}} P_i^{\mathrm{w}} + w^{\mathrm{s}} \sum_{i\in\mathcal{S}} \alpha_i^{\mathrm{s}} P_i^{\mathrm{s}} \quad (1)$$

subject to:

$$P_i^{\mathrm{g},c} + \big(1-\alpha_i^{\mathrm{w}}\big)P_i^{\mathrm{w}} + \big(1-\alpha_i^{\mathrm{s}}\big)P_i^{\mathrm{s}} - \big(1-\alpha_i^{\mathrm{d}}\big)P_i^{\mathrm{d}} - P_i^c = 0,\ \forall i\in\mathcal{B},\ \forall c\in\{0\}\cup\mathcal{C} \quad (2)$$

$$Q_i^{\mathrm{g},c} + Q_i^{\mathrm{s},c} + Q_i^{\mathrm{w},c} + b_i^{sh}(V_i^c)^2 - \big(1-\alpha_i^{\mathrm{d}}\big)Q_i^{\mathrm{d}} - Q_i^c = 0, \quad (3)$$

$\forall i\in\mathcal{B},\ \forall c\in\{0\}\cup\mathcal{C}$

$$P_i^c = \sum_{j:ij\in\mathcal{L}} r_{ij} e_i^c \big(b_{ij}^c f_j^c - g_{ij}^c e_j^c\big) - \sum_{j:ij\in\mathcal{L}} r_{ij} f_i^c \big(g_{ij}^c f_j^c + b_{ij}^c e_j^c\big) + \sum_{j:ij\in\mathcal{L}} g_{ij}^c (V_i^c)^2,\ \ \forall i\in\mathcal{B},\ \ \forall c\in\{0\}\cup\mathcal{C} \quad (4)$$

$$Q_i^c = \sum_{j:ij\in\mathcal{L}} r_{ij} e_i^c \big(g_{ij}^c f_j^c + b_{ij}^c e_j^c\big) - \sum_{j:ij\in\mathcal{L}} r_{ij} f_i^c \big(g_{ij}^c e_j^c - b_{ij}^c f_j^c\big)^4 - \sum_{j:ij\in\mathcal{L}} b_{ij}^c (V_i^c)^2,\ \ \forall i\in\mathcal{B},\ \forall c\in\{0\}\cup\mathcal{C} \quad (5)$$

$$\Big(g_{ij}^{c\,2} + b_{ij}^{c\,2}\Big)\Big[\big(f_i^c - f_j^c\big)^2 + \big(e_i^c - e_j^c\big)^2\Big] \le \big(I_{ij}^{\max}\big)^2, \quad (6)$$

$\forall ij\in\mathcal{L},\ \forall c\in\{0\}\cup\mathcal{C}$

$$V_i^{\min} \le V_i^{\mathrm{g},0} \le V_i^{\max},\ \ \forall i\in\mathcal{G} \quad (7)$$

$$V_i^{\mathrm{g},c} = V_i^{\mathrm{g},0},\ \forall i\in\mathcal{G},\ \forall c\in\mathcal{C} \quad (8)$$

$$V_i^{\min} \le V_i^c \le V_i^{\max},\ \ \forall i\in\mathcal{B}\setminus\mathcal{G},\ \forall c\in\{0\}\cup\mathcal{C} \quad (9)$$

$$f_i^c = 0,\ i\in\{\text{slack}\},\quad \forall c\in\{0\}\cup\mathcal{C} \quad (10)$$

$$P_i^{\min} \le P_i^{\mathrm{g},c} \le P_i^{\max},\ \forall i\in\mathcal{G},\ \forall c\in\{0\}\cup\mathcal{C} \quad (11)$$

$$|P_i^{\mathrm{g},c} - P_i^{\mathrm{g},0}| \le \Delta P_i^{\mathrm{g}},\quad \forall i\in\mathcal{G},\ \forall c\in\mathcal{C} \quad (12)$$

$$Q_i^{\min} \le Q_i^{\mathrm{g},c} \le Q_i^{c,\max},\quad \forall i\in\mathcal{G},\ \forall c\in\{0\}\cup\mathcal{C} \quad (13)$$

$$Q_i^{c,\max} = \min\begin{cases}\sqrt{\Big(\frac{V_i^{\mathrm{g},c}E_{f,i}^{\max}}{X_i^g}\Big)^2 - \big(P_i^{\mathrm{g},c}\big)^2} - \frac{(V_i^{\mathrm{g},c})^2}{X_i^g}\\ \sqrt{\big(V_i^{\mathrm{g},c}I_i^{s,\max}\big)^2 - \big(P_i^{\mathrm{g},c}\big)^2},\end{cases}$$

$\forall i\in\mathcal{G},\ \forall c\in\{0\}\cup\mathcal{C}$ (14)

$$Q_i^{\min} \le Q_i^{\mathrm{s/w},c} \le Q_i^{\max},\quad \forall i\in\{\mathcal{W},\mathcal{S}\},\ \forall c\in\{0\}\cup\mathcal{C} \quad (15)$$

$$0 \le \alpha_i^{\mathrm{w/s/d}} \le 1,\quad \forall i\in\{\mathcal{W},\mathcal{S},\mathcal{D}\} \quad (16)$$

where c represents the system state ($c=0$ denotes the intact state, or base-case, prior to the occurrence of a contingency and $c\ge 1$ denotes a post-contingency state).

The objective function (1) comprises the cost of conventional active power generation with (pseudo-)costs accounting for demand, wind, or solar generation shedding; such shedding decisions should be avoided as far as possible.

Equality constraints (2)–(3) express the active and reactive power balance equations, including the power flows through branches written explicitly in (4)–(5). Bounds on branch currents and bus voltage magnitudes are represented by (6)–(9). Constraints (10) set the angle phase reference in all states. Constraints (11) impose limits on active power for all generators in all states. Constraints (12) model the ramp-up and ramp-down limits on the generators in *"corrective mode"*. Constraints (13) model reactive power limits of generators. The field and armature winding heating limits are imposed by (14). The reactive power capability of wind and solar farms is limited by (15). Constraint (16) expresses the fact that one can only shed as much (wind, solar, demand) power as it is actually available. All variables in this constraint are contingency-independent for the sake of relieving computational burden as well as because: (i) α_i^d is just a measure to identify if the SCOPF problem becomes (physically) infeasible, fact revealed by a non-zero amount of load shedding, and (ii) their high cost in the objective function (1) discourages such curtailments.

Note that constraints (8) reflect the current industrial operation practice in many countries (e.g., in Europe), where each generator, as long as it has enough RPRs, has to maintain the same voltage set-point, agreed usually on a long-term basis, in both normal operation and after contingencies. This is because, after contingency, the operator does not have the necessary time

to act in optimizing and broadcasting another set of voltage set-points to generators.

3) Minimizers RPR-P and RPR-A

Reactive power is not yet traded in the market, despite previous research efforts to establish such markets [25]. However, power plants in Europe are remunerated for the ancillary service of voltage control (i.e., for providing an adequate amount of RPRs) to control voltage set-points instructed by the TSO. Furthermore, this remuneration is a matter of further research in several countries (e.g., Belgium [26], UK [27]) in the context of the large share of RES. Still, as argued, not the entire physical RPR is practically useful and deserves remuneration; only the necessary reserve is worthy. Our minimizers compute the overall amount of necessary RPRs, which can be valuable information to the TSO to understand how much RPR and from which generators should be procured, show the true capabilities of the system, and can inform on weak areas (those where the necessary reserves get large and RPRs become scarce).

The two minimizers, RPR-P and RPR-A, achieve the minimum overall necessary RPRs in production and absorption modes, respectively. The minimization of RPRs is performed at the optimal solution of the conventional SCOPF. It is essential to state that, unlike the conventional SCOPF, the two minimizers of overall necessary RPRs *do not compute any actual optimal active or reactive power re-dispatch*. Instead, without altering the cost-optimal settings of decision variables computed by the conventional SCOPF, these minimizers seek only *to assess* what is the *minimum overall amount of necessary RPRs* that meets system constraints under normal and contingency conditions.

Note however that, as demonstrated in [20], this objective cannot be obtained by post-processing SCOPF optimal solution. Indeed, the conventional SCOPF solution can be post-processed to calculate only the the reactive power required to ensure the power grid security, i.e. the *effective* RPRs, as $\max_{c\in\mathcal{C}}(Q_i^{\mathrm{g},c} - Q_i^{\mathrm{g},0}), \forall i \in \mathcal{G}$. According to the definition, the effective RPRs are generally much higher than the minimum amount of necessary RPRs, fully justifying the need for the proposed minimizers. In other words, the proposed minimizers will produce the minimum overall necessary RPRs, which are typically smaller than the summation of the maximum amount of reactive power reserve used by each generator across all contingencies at the conventional SCOPF solution, see Fig. 3.

Furthermore, the conventional AC SCOPF does not model the generator' switching between under voltage control and under reactive power limit [20], [28], i.e., at the optimum a generator can still be under voltage control and at a reactive power limit, which is inaccurate and prevents evaluating properly RPRs. In fact, research has been conducted for almost two decades on how to express, in a computationally reliably way in OPF, the reality that a generator can be either under voltage control or at a reactive power limit. This requirement has been modelled mathematically through complementarity constraints (CCs), see eqs. (21), in the seminal work [29]. However, despite its mathematical elegance, solving the resulting nonlinear programming optimization problem with many CCs is not numerically reliable [30] and there is no solver that can handle a significant number of CCs reliably numerically and be still scalable. Modeling this switching is one of the two AC SCOPF industrial needs to handle in the recent competition organized by ARPA-E [28]. Our modeling of generators switching is presented next.

Without loss in generality and to check if sufficient RPRs are available anytime, we consider two alternative operation modes (i.e., reactive power production vs absorption) in the RPRs evaluation, where the production mode is relevant especially at peak load conditions while the absorption mode is meaningful rather at the base/light load conditions.

The RPR-P SCOPF problem computes the necessary RPRs in production mode and is formulated as follows:

$$\min_{RQ_i^{\mathrm{g}}, P_i^{\mathrm{g},c}, Q_i^{\mathrm{g},c}, V_i^{\mathrm{g},c}} \sum_{i\in\mathcal{G}} RQ_i^{\mathrm{g}} \tag{17}$$

subject to: (2)–(6), (10)

$$P_i^{\min} \le P_i^{\mathrm{g},c} \le P_i^{\max},\ i \in \{\text{slack}\},\ \forall c \in \{0\}\cup\mathcal{C} \tag{18}$$

$$P_i^{\mathrm{g},c} = P_{i,\mathrm{imp}}^{\mathrm{g},0},\quad \forall i \in \mathcal{G}\setminus\{\text{slack}\},\ \forall c \in \{0\}\cup\mathcal{C} \tag{19}$$

$$V_i^{\mathrm{g},0} = V_{i,\mathrm{imp}}^{\mathrm{g},0},\quad \forall i \in \mathcal{G} \tag{20}$$

$$\alpha_i^{\mathrm{w/s/d}} = \alpha_{i,\mathrm{imp}}^{\mathrm{w/s/d}},\quad \forall i \in \{\mathcal{W},\mathcal{S},\mathcal{D}\} \tag{21}$$

$$Q_i^{\min} \le Q_i^{\mathrm{g},0} \le Q_i^{0,\max},\quad \forall i \in \mathcal{G} \tag{22}$$

$$0 \le RQ_i^{\mathrm{g}} \le Q_i^{c,\max} - Q_i^{\mathrm{g},0},\quad \forall i \in \mathcal{G},\ \forall c \in \{0\}\cup\mathcal{C} \tag{23}$$

$$Q_i^{\min} \le Q_i^{\mathrm{g},c} \le Q_i^{\mathrm{g},0} + RQ_i^{\mathrm{g}},\quad \forall i \in \mathcal{G},\ \forall c \in \mathcal{C} \tag{24}$$

$$Q_i^{c,\max} = \min\begin{cases} \sqrt{\left(\frac{V_i^{\mathrm{g},c}E_{f,i}^{\max}}{X_i^g}\right)^2 - \left(P_i^{\mathrm{g},c}\right)^2} - \frac{(V_i^{\mathrm{g},c})^2}{X_i^g} \\ \sqrt{\left(V_i^{\mathrm{g},c}I_i^{\mathrm{s,max}}\right)^2 - \left(P_i^{\mathrm{g},c}\right)^2}, \end{cases}$$

$$\forall i \in \mathcal{G},\ \forall c \in \{0\}\cup\mathcal{C} \tag{25}$$

$$V_i^{\min} - \delta \le V_i^c \le V_i^{\max},\ \forall i \in \mathcal{B}\setminus\mathcal{G},\ \forall c \in \mathcal{C} \tag{26}$$

$$V_i^{\min} - \delta \le V_i^{g,c} \le V_{i,\mathrm{imp}}^{\mathrm{g},0},\ \forall i \in \mathcal{G},\ \forall c \in \mathcal{C} \tag{27}$$

where $0 \le \delta \le 0.1$ is a parameter aimed to relax the voltage limits so as to stimulate a smaller usage of the reactive power reserves, and new variables RQ_i^{g} denote the necessary reactive power reserve of conventional generators, measured with respect to their base case reactive power production $Q_i^{\mathrm{g},0}$, see (23) and (28). Constraint (25) represents the reactive power maximum limit using a proper modeling of the generators' capability curves.

Note that *several quantities are frozen at the optimal SCOPF solution* (i.e., parameters defined by subscript $\bullet_{\mathrm{imp}}$) as shown in constraints (19)–(21). Furthermore, in (18), only one (slack) generator compensates for active power mismatch after contingency. This is a simple and typical assumption in preventive mode, further motivated by the fact that the solution of the conventional SCOPF (generators optimal re-dispatch in normal operation and after each contingency) acts as fix input to the two evaluators RPR-P and RPR-A and thus there is only a minor variation in losses due to the minimization of needed reserves and possible voltage drops. We observed in all the simulations that the change in active power of the slack generator is minor and hence the approximation is reasonable. Still, a more refined generators' share of losses variation is possible.

Constraints (22) limit the reactive power of the conventional generators in the base case, while constraints (23)–(24) enable defining and evaluating the RPRs. Inequality constraints (26)

express the limits on the voltage of non-generator buses, and constraints (27) allow generator voltages to drop from the imposed value after a contingency (switching) if this can reduce the overall amount of necessary RPRs. We thus approximate the CCs expressing that a generator can be either under voltage control or at a reactive power limit, in reactive power production mode (the argumentation is similar for absorption mode), with the set of constraints (23)–(24) and (27). We observed empirically in all simulations that constraint (27) always holds at optimum as equality for generators which did not reach a reactive power limit and it is below the setpoint if the generator is in the limit. In other words, for our problem, when a generator reaches a reactive power limit, empirically, thanks to the intrinsic nature of the problem, the voltage deviates (in this case drops) from the desired voltage setpoint. This is due to the fact that, under loaded operating conditions and after contingency (i.e. where reactive power production matters), the higher the generator voltage, the larger the generator reactive power output, the smaller the reactive power losses, the smaller the generators reactive power response in a scenario and hence the smaller the needed RPRs.

Knowing the minimum amount of RPRs could be exploited to develop financial compensation schemes valuating these reserves. Accordingly, to stimulate generators' response to a maximum, RPRs minimizers allow under contingencies generators' voltage to deviate from the imposed value, e.g., to drop in production mode (see (27)) or to increase in absorption mode (see (32)), if this can improve the value of the objective function as well as to simulate generator switching between under voltage control or under reactive power limit.

The RPR-A SCOPF problem is formulated in a similar way to the RPR-P problem, except that constraints (28)–(32) replace the set of constraints (23)–(27):

$$0 \leq RQ_i^{\mathrm{g}} \leq Q_i^{\mathrm{g},0} - Q_i^{\min},\ \forall i \in \mathcal{G} \tag{28}$$

$$Q_i^{\mathrm{g},0} - RQ_i^{\mathrm{g}} \leq Q_i^{\mathrm{g},c} \leq Q_i^{c,\max},\ \forall i \in \mathcal{G},\ \forall c \in \mathcal{C} \tag{29}$$

$$Q_i^{c,\max} = \min \begin{cases} \sqrt{\left(\frac{V_i^{\mathrm{g},c} E_{f,i}^{\max}}{X_i^g}\right)^2 - \left(P_i^{\mathrm{g},c}\right)^2} - \frac{(V_i^{\mathrm{g},c})^2}{X_i^g} \\ \sqrt{\left(V_i^{\mathrm{g},c} I_i^{s,\max}\right)^2 - \left(P_i^{\mathrm{g},c}\right)^2}, \end{cases}$$

$$\forall i \in \mathcal{G},\ \forall c \in \{0\} \cup \mathcal{C} \tag{30}$$

$$V_i^{\min} \leq V_i^c \leq V_i^{\max} + \delta,\ \forall i \in \mathcal{B} \setminus \mathcal{G},\ \forall c \in \mathcal{C} \tag{31}$$

$$V_{i,\mathrm{imp}}^{\mathrm{g},0} \leq V_i^{g,c} \leq V_i^{\max} + \delta,\ \forall i \in \mathcal{G},\ \forall c \in \mathcal{C}. \tag{32}$$

It is important to mention that when the conventional SCOPF is feasible, the RPR minimization problems are also feasible. This is due to the fact that in the RPR problems the conventional generator voltage limitations under contingencies are relaxed, while other variables are merely frozen to their optimal value obtained in the conventional SCOPF problem.

4) The Optimal Reactive Power Dispatch (ORPD) Module

The ORPD module seeks the best settings for transformers ratio, shunt capacitors/reactors, and generators' voltage that maximize the *physical* RPRs in either production or absorption modes. The problem is formulated in production mode as follows:

$$\max_{\substack{P_i^{\mathrm{g},c}, Q_i^{\mathrm{g},c}, V_i^{g,c} \\ r_{ij}, b_i^{sh}, \alpha_i^{\mathrm{w/s/d}}}} \sum_{i \in \mathcal{G}} (Q_i^{0,\max} - Q_i^{\mathrm{g},0}) + w^{\mathrm{d}} \sum_{i \in \mathcal{D}} (1 - \alpha_i^{\mathrm{d}}) P_i^{\mathrm{d}} + w^{\mathrm{w}} \sum_{i \in \mathcal{W}} (1 - \alpha_i^{\mathrm{w}}) P_i^{\mathrm{w}} + w^{\mathrm{s}} \sum_{i \in \mathcal{S}} (1 - \alpha_i^{\mathrm{s}}) P_i^{\mathrm{s}} \tag{33}$$

subject to: (2)–(16)

$$r_{ij}^{\min} \leq r_{ij} \leq r_{ij}^{\max},\quad \forall ij \in \mathcal{L} \tag{34}$$

$$b_i^{\min} \leq b_i^{sh} \leq b_i^{\max},\quad \forall i \in \mathcal{B} \tag{35}$$

where $r_{ij}^{\min}$/$r_{ij}^{\max}$ and $b_i^{\min}$/$b_i^{\max}$ are the lower and upper bounds of transformer ratio and shunt susceptance, respectively.

C. The Outer Loop for Long-Term Operation

1) The Aim

The inner loop for day-ahead operation, with its four AC SCOPF modules, constitutes the computation core of the proposed methodology. Although adequate for its time frame, the inner loop alone is insufficiently refined to assess RPRs in long term. To this end, to broaden the scope of the methodology beyond the current hourly resolution of short-term operation, the goal of the outer loop is to evaluate in a realistic manner RPRs, i.e., by using different plausible assumptions, in two longer time-frames: 1-year ahead or $y^{\max} \leq 5$ years ahead with a time resolution of $\Delta y \geq 1$ years, see Fig. 1. Still, the various choices made in the outer loop act essentially as different input data in the computation modules of the inner loop.

2) 1-year ahead operation

For the specific evaluation of RPRs, the 1-year ahead operation is mimicked for a number $d^{\max}$ of representative days of that year, e.g., defined as a combination of day-type based on the season (spring, summer, autumn, and winter) and day of the week (weekdays or weekend). In the construction of data for such days, one can use any statistical method that exploits existing weather historical seasonal data on wind speed and solar irradiance, including their correlation. These can underpin the estimation of wind speed forecast and solar irradiance and convert them into wind power and solar power, respectively, depending on the foreseen technology to be deployed. For each such defined day d we consider: (i) a forecasted load profile with the hourly resolution, (ii) a forecast of RES production using the ARIMA model, and (iii) the topology of the system i.e., generators online and connected branches. Regarding the latter aspect, in absence of a unit commitment program, the optimistic assumption that all generators are online anytime is made, although their active power dispatch is adapted to the total load. It is also assumed that all branches are connected anytime.

3) $y^{\max}$-years ahead operation

This time frame entails the definition of energy transition scenarios toward renewable-dominated electricity supply in the next years, e.g., up to 2050. However, as already discussed we suggest that the proposed methodology can be applied to the current situation for 5 years ahead. Then, after 5 years, the system state and its development plans are updated, and the methodology is repeated for the next 5 years and so on up to 2050. Therefore, the proposed methodology will not be applied

or cover the energy transition up to 2050 in one shot but applied repeatedly for smaller time horizons (e.g., 5 years).

The main task during each time period of the energy transition consists in defining a set of big mutations in terms of phasing out of the large fossil-fuel-based power plants (FFPPs) and their displacement by RES. As such, several plausible sequences of taking FFPPs out of service are defined based on their lifetime and environmental targets adopted by countries among others.

We further assume different locations, types, and sizes for deployed RES that displace FFPPs. A key assumption is that the lost FFPPs active power is compensated through power injections from RES connected in distribution networks, hence reducing the net active power consumption drawn from the transmission system at that node, while new RES deployed in the transmission system is considered independently. In absence of more precise information, two variants for compensating for the lost active power are considered:

1) *variant 1*: it replaces the active power of each phased-out generator with renewable energy production operating at the unitary power factor at the same bus, as in [4];
2) *variant 2*: it distributes the lost active power on load buses, decreasing the active power of loads proportionally to their active power consumption at peak load as:

$$P^{\mathrm{d}}_{i,\mathrm{new}} = P^{\mathrm{d}}_{i,\mathrm{old}} - P^{g}_{k,\mathrm{phasedout}}\left(P^{\mathrm{d}}_{i,\mathrm{peak}} \times \sum_{j\in\mathcal{D}} P^{\mathrm{d}}_{j,\mathrm{peak}}\right) \qquad (36)$$

where $i \in \mathcal{D}$ and $k \in \mathcal{G}$, subscripts $\bullet_{\mathrm{new}}$ and $\bullet_{\mathrm{old}}$ refer to the old and new values of the demand at bus i, and $\bullet_{\mathrm{peak}}$ denotes the peak demand over a 24-hour time frame.

Finally, the forecast of the load profile will rely on a typical assumption of a slight load increase per year, proportionally with the current peak load at each node.

The outer loop can accommodate straightforwardly any other system change known by the TSO (e.g., generation or network expansion) as discussed in subsection III-H.

III. Numerical Simulation Results

A. Description of the Test Systems and Simulations Assumptions

This section showcases extensively and without loss of generality the most important features of the proposed methodology on the Nordic32 test system [4], [31]. Then, it briefly assesses its computation performance on a large 1,203 test system [20].

The Nordic32 system, see its one-line diagram in Fig. 2, is a realistic model of the (60 nodes, 23 generators) Swedish power system. Unless otherwise specified, the postulated set of contingencies is composed of 33 single line outages as in [4].

The second test system is the modified planning version of the (1,203 buses, 177 generators) RTE France from mid 90's [20]. Four sets of 5, 10, 15, and 20 critical contingencies, respectively, including loss of lines and generators, are considered.

All simulations have been performed in the open-source Julia/JuMP programming language [32], resorting to IPOPT [33] to solve all AC SCOPF problems. The computation times provided have been obtained on a PC with an Intel 10th generation i7 processor, 2.30-GHz, and 48GB of RAM.

All SCOPF problems impose the same voltage limits of 0.9 p.u.–1.1 p.u. in a normal state. Conventional SCOPF uses the same voltage range also under contingencies. The RPR-P and RPR-A SCOPF problems relax the voltage limits in post-contingency states, using $\delta = 0.1$ p.u. in (26)–(27) and (31)–(32), setting accordingly a lower bound of 0.8 p.u. (for RPR-P SCOPF) and an upper bound of 1.2 p.u. (for RPR-A SCOPF), respectively.

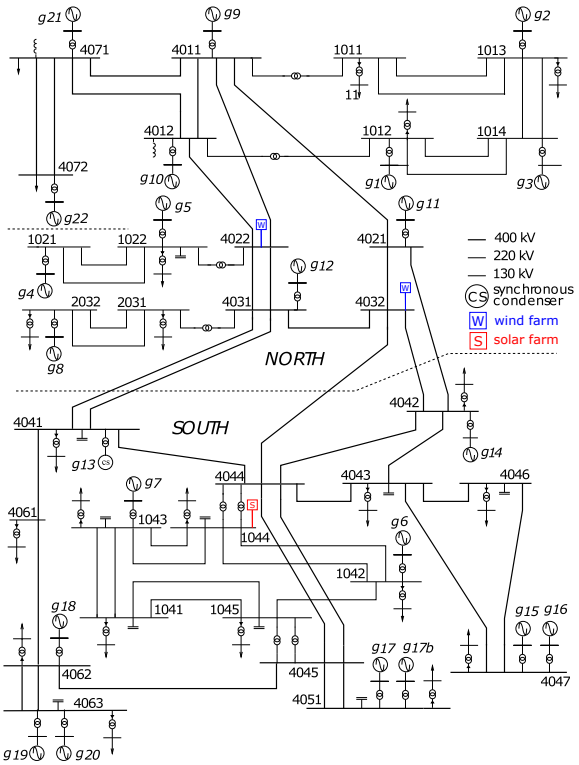

Fig. 2: One-line diagram of the modified Nordic32 system.

From now on, the impact of various aspects of the proposed methodology on the value of RPRs is studied, which will clearly showcase the significant extension of the preliminary work [4].

B. Necessary RPRs vs. Effective RPRs

Fig. 3 provides a representative sample, obtained after phasing out g14, g16, and g18, of the difference between the necessary and effective RPR of each generator. One can observe that for the majority of generators the effective RPR is larger than necessary RPR. For some generators (e.g., g2, g9, g21) the necessary RPR is zero. This outcome is due to a good concentration of generators in those regions, that can compensate for each other the absence of some reserve in one generator. These differences translate into an overall effective RPRs amounting to 1.85 Gvar, that is larger than the overall necessary RPRs, which is equal to 1.65 Gvar. This means that the computation of necessary RPRs leads to a reduction of RPR usage of 0.20 Gvar, justifying the importance of the proposal.

C. Impact of MW-compensation on the RPRs

In what follows, unless stated otherwise, the Nordic32 system is considered for the sake of complete illustration of the methodology proposed in Section II. A simple energy transition

This article has been accepted for publication in IEEE Transactions on Power Systems. This is the author's version which has not been fully edited and content may change prior to final publication. Citation information: DOI 10.1109/TPWRS.2022.3216639

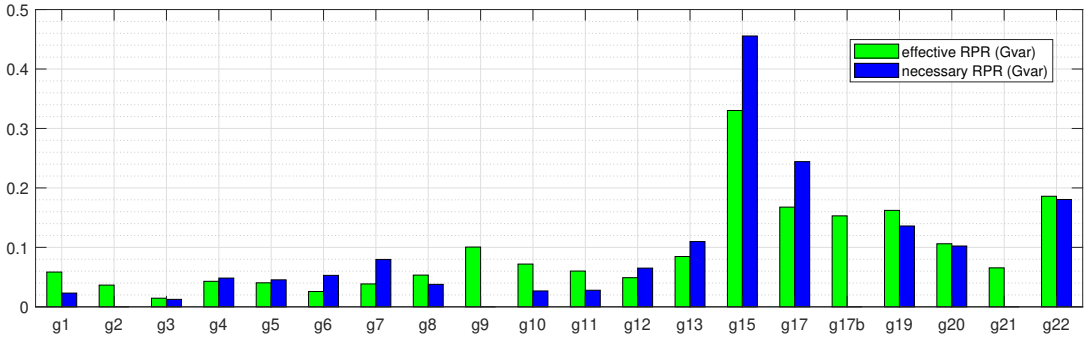

Fig. 3: The necessary and effective RPRs for each generator.

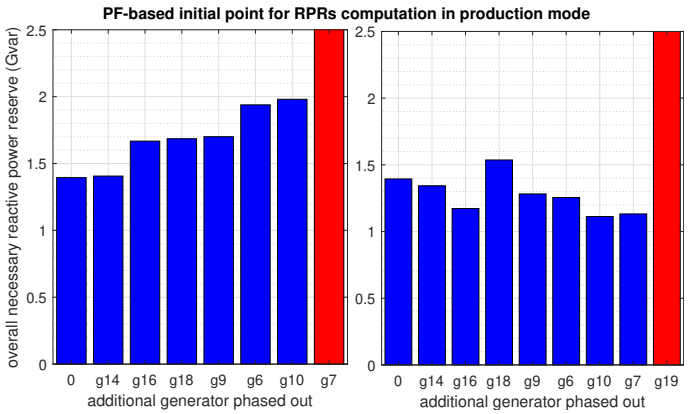

Fig. 4: Overall necessary RPRs in production mode, compensating active power via first variant (left-plot) – second variant (right-plot).

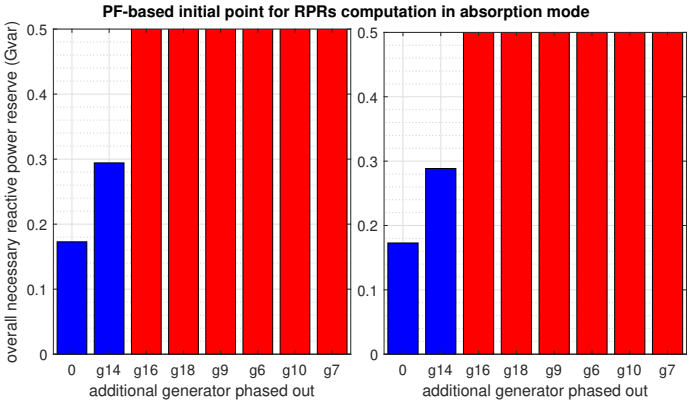

Fig. 5: Overall necessary RPRs in absorption mode, compensating active power via first variant (left-plot) – second variant (right-plot).

scenario is assumed, which consists in phasing out sequentially fossil-fuel generators and compensating the lost MW with power injections from distribution networks, using the variants 1 and 2 described in section II-B3.

Note that, for the sake of comparison with [4], after phasing out a generator and compensating the active power using one of the above variants, we perform an AC *power flow* (PF) computation to determine the new operating point as input of SCOPF-based RPRs minimizers.

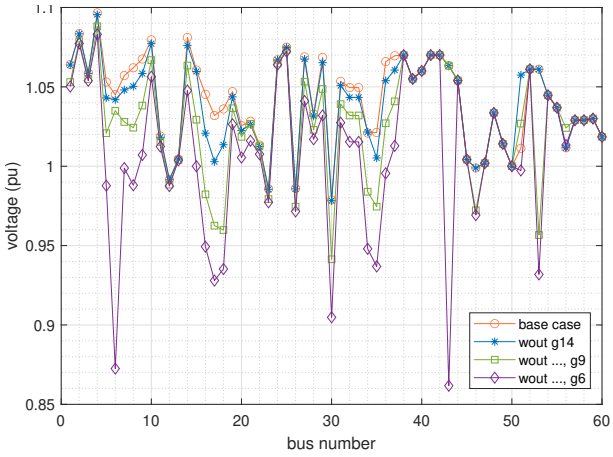

Fig. 6: Bus voltages as generators are phased out.

Figs. 4 and 5 compare the two MW compensation variants in production and absorption modes, corresponding to peak load (i.e., around 9 GW and 3.6 Gvar) and light load[1] cases, respectively. The left-hand side and right-hand side plots correspond to the results for variant 1 (incidentally this is the only energy transition result presented in [4]) and variant 2, respectively. The blue boxes and red boxes indicate feasible and infeasible SCOPF problems, respectively. Infeasibility occurs due to the scarcity of RPRs, as the system is weakened by removing generators from service.

1) Production mode analysis

For the sequence of generators shown in the left plot of Fig. 4, Fig. 6 depicts the decay in voltages, for a relevant critical contingency, as generators are progressively phased out. The figure suggests that the RPRs of the remaining generators cannot prevent the decay of voltages to low values causing the AC SCOPF problem to become infeasible.

To support the interpretation of these RPRs results, table I provides the active and reactive power losses at the initial operating point where RPRs are assessed, after phasing out each generator of the assumed sequence.

The left plot of Fig. 4 shows that the requirement of RPRs

[1]Light load is assumed as 60% of the peak load.

This article has been accepted for publication in IEEE Transactions on Power Systems. This is the author's version which has not been fully edited and content may change prior to final publication. Citation information: DOI 10.1109/TPWRS.2022.3216639

TABLE I: Active and reactive power losses in production mode for the two compensation variants.

scenarios	compensation			
	variant 1		variant 2	
	active loss (MW)	reactive loss (Mvar)	active loss (MW)	reactive loss (Mvar)
base	139.97	-2234.32	139.97	-2234.32
g14	139.42	-2347.86	138.93	-2393.13
g16	140.25	-2311.46	133.29	-2508.98
g18	140.01	-2338.52	149.42	-2383.31
g9	140.67	-2316.56	121.54	-2735.97
g6	142.86	-2249.43	128.91	-2645.42
g10	143.98	-2216.16	105.54	-2949.10
g7	-	-	111.40	-2913.27

when using the variant 1, increases monotonically and often substantially. This is corroborated with the results reported in table I, which indicate that as the number of fossil-fueled generators taken out of service grows, the active power losses increases. This is an expected behaviour, because the active power of generators phased out is fully compensated at the same buses while, at the same time, the system is deprived of the full reactive power of these generators. This stresses the system and calls for reactive power reserve support from remote generators until the voltage constraints cannot be anymore satisfied and the SCOPF problems become infeasible.

Further, the behavior of RPRs using variant 2, shown in the right plot of Fig. 4, indicates a generally decreasing trend before reaching infeasibility. This is apparently counter-intuitive and cannot be easily predicted. This plot indicates that the overall necessary RPR is not consistently increasing and taking more generators out of the service does not always stress the system. Indeed, as table I indicates, active power losses are rather oscillating than having a steady increasing trend, which means that, despite phasing out of a generator, the active power compensation can have a stronger effect and relieve the grid and need for reserves. This grid-relieving effect is also confirmed in the figure since in variant 2 the grid resists phasing out one more generator (e.g., g7) than in variant 1.

This counter-intuitive example indicates that the break-point where the RPRs become insufficient, and hence planning for providing additional reactive reserves is inevitable, cannot be estimated by the TSO through simple trend indicators, as for variant 1. It further highlights the value of our approach to inform TSOs in cases where the RPRs scarcity and requirements are difficult to predict. Therefore, our variant of phasing out generators enables simulating until the last point where the RPRs are still sufficient.

2) Absorption mode analysis

Fig. 5 compares the MW compensation variants in absorption mode. The latter corresponds to light/low load. The figure shows a clear increasing need for RPRs as one removes generators. One can observe that RPRs become insufficient at the same time in both variants and the graphs of both variants look similar, albeit there are some small differences in the values of RPRs. This resemblance is attributable to the insignificant effect of the compensation method on the highest voltages that are prone to violate their limit. However, further experiments are necessary to ascertain if this outcome can be generalized.

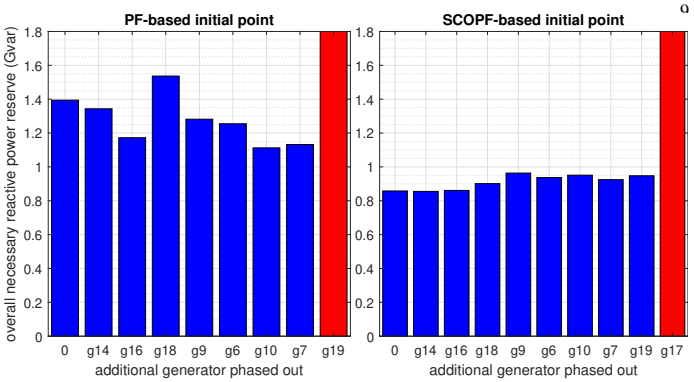

Fig. 7: Overall necessary RPRs in production mode: initial point based on AC PF (left-plot) – AC SCOPF (right-plot).

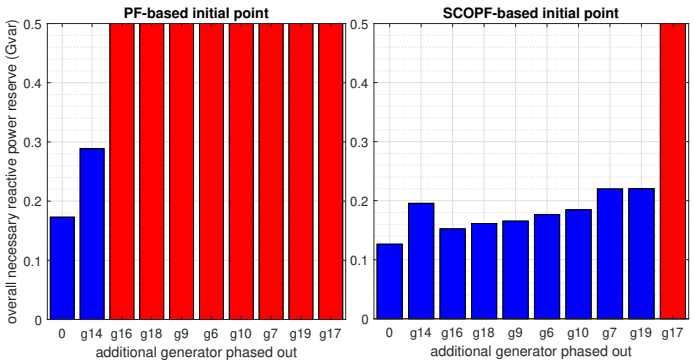

Fig. 8: Overall necessary RPRs in absorption mode: initial point based on AC PF (left-plot) – AC SCOPF (right-plot).

The figure indicates that RPRs become insufficient rapidly, after phasing out only two generators, and the absorption capability is much more constraining than the production capability (see Fig. 4).

D. Impact of Initial Operating Point Computation on the RPRs

Continuing with the variant 2 for MW compensation, the realism and modelling improvement of embedding optimal grid operation, via the conventional AC SCOPF, in the proposed methodology (to fed RPRs minimizers) is highlighted and compared to the mere AC PF computation in [4].

From Figs. 7 and 8 one can note, thanks to the use of SCOPF including for the optimization of voltage profile, that: (i) the RPRs needs considering conventional AC SCOPF are significantly smaller than those using PF and (ii) SCOPF is more effective than PF in delaying (with seven generators phased-out) the occurrence of RPRs scarcity. In addition, the use of SCOPF leads to a visible general trend of the growing need for RPRs as generators are removed.

E. Impact of the Set of Contingencies on the RPRs

In this experiment, 19 *generator outages* are considered together with the 33 $N-1$ line contingencies from [4], i.e., in total 52 contingencies. To enable a fair comparison with [4], variant 1 for MW compensation is used. The RPRs in production and absorption modes are displayed in Fig. 9. In

This article has been accepted for publication in IEEE Transactions on Power Systems. This is the author's version which has not been fully edited and content may change prior to final publication. Citation information: DOI 10.1109/TPWRS.2022.3216639

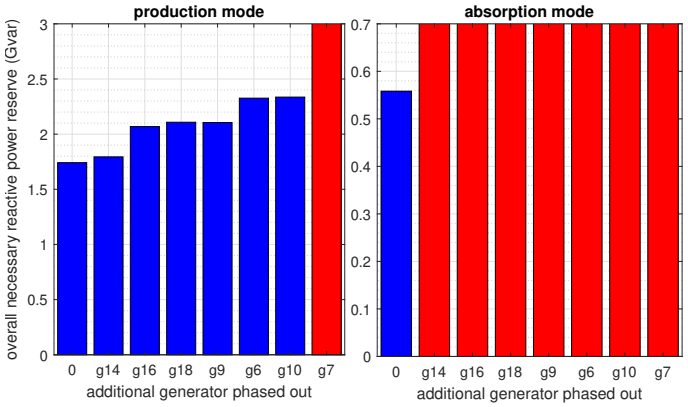

Fig. 9: Overall necessary RPRs in production and absorption modes considering both line and generator contingencies.

production mode, when comparing the left-plot in this figure with the left-plot in Fig. 4, one can remark that including (as required by TSO practical needs) also generators contingencies do not change the RPRs break-point but only, as expected, significantly increases the overall necessary RPRs. However, we consider this a case-dependent outcome and expect that, as generators impose additional constraints, the RPRs break-point is encountered earlier than with only line contingencies. This assertion is confirmed by looking at RPRs in absorption mode in Fig. 9 (right-plot) and 5 (left-plot); one can observe that, when generators contingencies are included, the RPRs become insufficient immediately. This is owing to the unusually high reactive power produced by lines at light load (notice from table I that reactive power losses are negative even at peak load), which cannot be absorbed under generator contingencies without creating over-voltages.

These experiments clearly underline the superior and more realistic modeling capability of the proposed methodology than in [4], which overestimated the RPRs breaking-point.

F. Full Illustration of the Proposed Methodology

1) Results for the Inner and Outer Loops

The full methodology is now illustrated on a futuristic renewable-dominated version of the Nordic32 test system, in which, during the assumed energy transition scenario, two identical large wind farms of 1000 MW rated power are deployed at nodes 4022 and 4032 as well as one solar PV farm of 500 MW rated power is installed at node 1044, see Fig. 2. The sequence of generators phased out shown in Fig. 10 is assumed, where one additional generator is phased-out, without loss of generality, every year. The lost MWs are compensated by RES deployed in distribution systems via variant 2 and the three additional RES connected directly to the transmission system.

To factor in the uncertainty of the renewable production, for illustration purposes, the auto regressive integrated moving average model (ARIMA) [22], [23] has been used to generate realistic wind and solar power production scenarios. Given the planning stage, only $sc = 10$ different RES scenarios for each considered typical day have been generated, see Fig. 10.

The average daily load patterns for four different typical days (modelling a: winter working day, winter weekend, summer working day, and summer weekend), adopted from [34], have been used. However, for illustrative purposes and space limits, the results are shown only for a typical summer workday.

We pursue considering the list of 52 $N-1$ contingencies, comprising 19 generators and 33 lines.

Figs. 10 and 11 report the overall necessary RPRs, in production and absorption modes, for the energy scenario transition described above until the calculated break down.

Each individual subplot in these figures corresponds to the necessary RPRs in production and absorption modes for every hour of the next day. Each hour includes 10 RES power production scenarios and every scenario is shown by a bar using the same color in all subplots. Such a subplot corresponds to the inner loop and is the proposed way to support the TSO in day-ahead operation to ascertain whether RPRs are sufficient for the next day. Since these results are obtained at the planning stage, more accurate forecasts of load profile and RES generation in day-ahead operation have to be used in the methodology.

One can remark in specific hours some spikes in the RPRs needs, which are due to the RES-induced generation pattern and also AC SCOPF optimization of the initial point. Therefore, due to these two reasons, for a given day, the highest need for RPRs does not coincide with the peak load in the evening but occurs more often around noon (see the first three subplots in both figures).

The creation via AC SCOPF of the initial points where RPRs are evaluated is the key determinant of the RPRs daily values during the energy transition. *Because AC SCOPF does not optimize the RPRs but optimizes only the cost of re-dispatch to maintain $N-1$ security with respect to voltage and thermal limits, accordingly, weakening (in general) the system by shutting down generators does not necessarily worsen (i.e., increase) the needs for RPRs. This is the major explanation for all results presented throughout the paper.* For example, this is the main explanation of why, as generators are phased out (in critical areas, e.g. the South, for the voltage support of the grid), the necessary RPRs do not increase monotonically or significantly but present a rather ambiguous trend: the AC SCOPF still finds the best use of resources to sustain the grid voltage profile. Consequently, the severity of the situation is masked until late, e.g., after phasing out the fifth generator (g19). This underpins the value of the proposed methodology to pursue the computation until identifying the RPRs breaking point.

The same explanation sustains also the observation that, although the first RPRs issue is identified when phasing out g19, after shutting down also g7, the time of scarce RPRs widens. Note also that g19 is not among the most prominent generators for sustaining the voltage profile in the critical areas; thus, combined with the MW compensation, this may actually also relieve the grid stress.

Let us remind that the scarcity of RPRs is declared with the AC SCOPF problem becomes (physically) infeasible, this fact is identified by a non-zero amount of load shedding, see objective (1). In this context, another important observation is

This article has been accepted for publication in IEEE Transactions on Power Systems. This is the author's version which has not been fully edited and content may change prior to final publication. Citation information: DOI 10.1109/TPWRS.2022.3216639

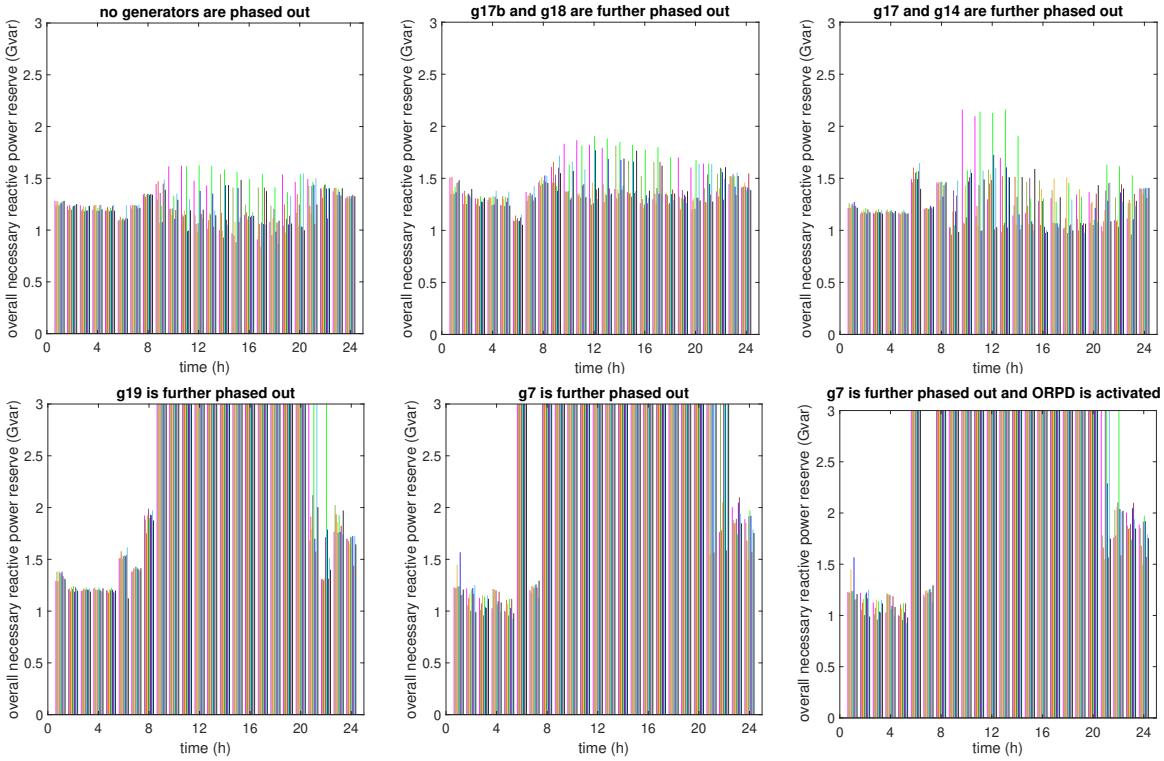

Fig. 10: Necessary reactive power reserve in production mode as generators are phased out for a typical summer workday.

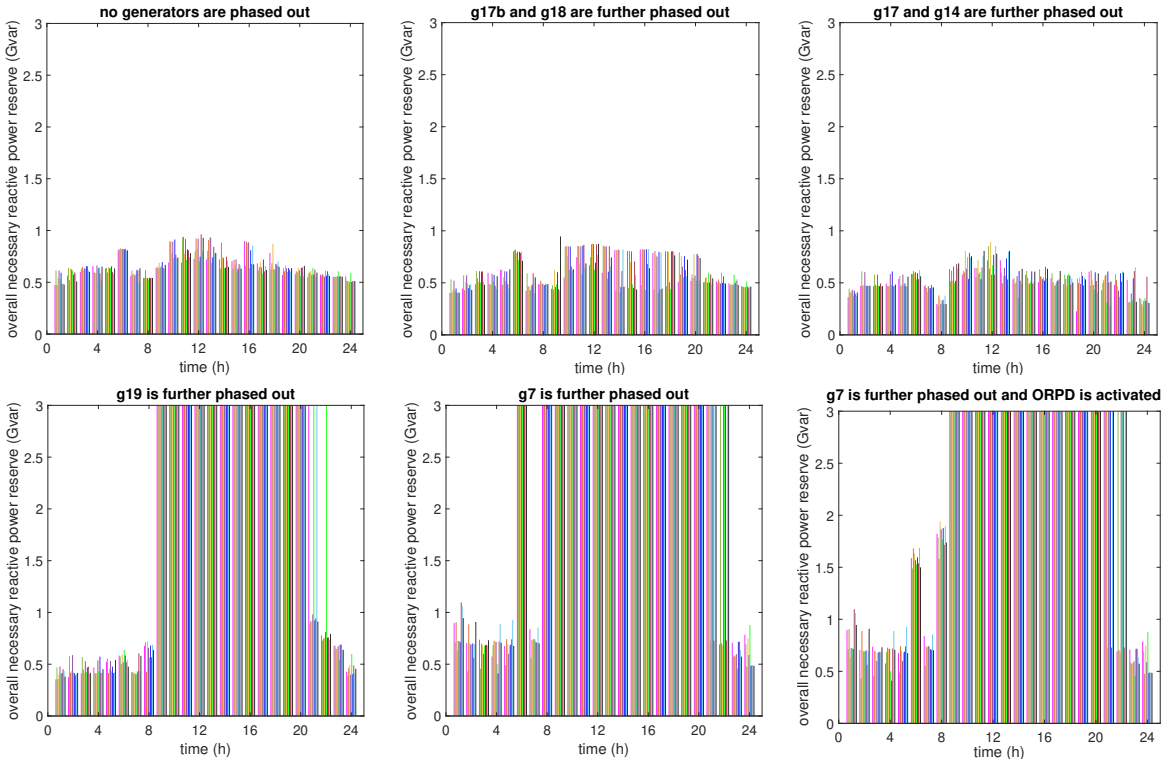

Fig. 11: Necessary reactive power reserves in absorption mode as generators are phased out for a typical summer workday.

that, albeit prior to phasing out of the 4-th generator the available reserves seem adequate, by continuing phasing out generators achieving feasible solutions without load shedding is impossible. The subplots after 4 and 5 generators are phased out (see the second row in Figs. 10 and 11) indicate that the necessary RPRs are obtained by resorting to load shedding. Following the phasing out of more than 4 generators, RPRs scarcity unfolds severely as SCOPF provides physically infeasible solutions (i.e., load shedding is activated) in a large number of scenarios.

Another important outcome of the proposed methodology is the interpretation of the degree of RPRs scarcity. For example, the RPRs are alarmingly scarce in more than 51% of the scenarios in the subplot corresponding to the phasing out of g19. This can be already considered as the RPRs break-point, after which phasing out of g7 worsens the situation as 64% of the scenarios are infeasible and hence have insufficient RPRs. These figures can be very useful in supporting the TSO to determine where countermeasures have to be planned. For instance, if a case with a few scenarios where RPRs are scarce could be tolerated, the extreme situation of phasing out g19 and even more g7 requires carefully strengthening the var support of the grid.

Clearly, although another sequence of generators phased out may result in distinct RPRs, the evidence gathered so far allows arguing that the overall necessary RPRs will not necessarily consistently increase with the number of phased-out generators.

Finally, the last subplots (second row, at the right) of Figs. 10 and 11 show the impact of the ORPD module on the overall necessary RPRs after phasing out of 6 generators. Thanks to more degrees of freedom (e.g., variable transformers ratio, shunt elements), ORPD can remove the SCOPF infeasibility and load shedding, hence ensuring RPRs sufficiency in some hours, e.g. hours 21 and 22 in the last subplot of Fig. 10, and hours 6 and 8 in the last subplot of Fig. 11. Furthermore, the ORPD reduces by 21% on average the amount of load shedding in infeasible cases. However, in this case, the impact of the ORPD module is marginal and it is not able to postpone the occurrence of RPRs scarcity.

Further, in terms of computation effort, the average time needed to solve the three problems (the conventional SCOPF optimization and RPR-P and RPR-A SCOPF problems, all including 52 $N-1$ contingencies) is about 67.5s for each scenario. This computational effort is clearly affordable by operators even in the operation planning stage.

G. Computation Effort on a Large-Scale Power System

This section ascertains the computation performance of the most computationally intense modules of the proposed methodology on the RTE grid model introduced in section III-A.

Table II yields the results of RPR-P and RPR-A SCOPF problems for four sets of $N-1$ critical contingencies including 5 lines, 10 lines, 10 lines, and 5 generators, and 10 lines and 10 generators, respectively. RPR-P and RPR-A problems consider peak load and low load (set to 80% of the peak load) conditions, respectively. One can remark that line contingencies have a stronger impact on RPRs in production mode, while generator contingencies are much more demanding in absorption mode.

TABLE II: RPRs and CPU time for four sets of critical contingencies.[12]

1203-bus system				
$\|\mathcal{C}\|$	RPR-P (Mvar)	time (s)	RPR-A (Mvar)	time (s)
5	1773.76	51.8	60.06	39.8
10	2242.20	133.9	140.56	91.3
15	2550.04	164.1	1659.43	162.9
20	2601.55	201.3	1804.98	291.7

As expected, both the necessary RPRs and computation effort grow with the problem size. However, *largest computation effort of the SCOPF problems is still rather light and does not prevent contemplating the application of the proposed methodology in day-ahead operation.*

H. Discussion on Further Refinements and Practical Applicability of the Proposed methodology

The modeling of the energy transition is a complex, country-specific process. Accordingly, this subsection discusses briefly several aspects related to the proposed methodology that could be further refined or may change during the planning time horizon but also in short-term operation planning.

In the day-ahead operation time frame, a security-constrained unit commitment (UC) [35] (e.g., in the US energy markets) or energy market clearing process (e.g., in Europe) is performed and informs, as input data, our methodology about the online generators and their market-desired production in each hour of the next day. If the outcome of the energy market clearing does not satisfy voltage constraints, the TSO has to run the day-ahead AC SCOPF (in Europe) or security-constrained economic dispatch (in the US) [36], [37] in order to procure adequate reactive power reserves for voltage control ancillary service. As the voltage issues are rather local, the TSO may require the start-up of some generators (called "must-run"), initially determined as off-line after the market clearing. In the worst case, all initially off-line generators can be started-up to support volatile voltage profiles, which is our pessimistic assumption as we seek to identify when RPRs become scarce. Then, the assets planned for maintenance (network, generators) for the next day are known by the TSO. These aspects can be straightforwardly modelled in our methodology as input parameters.

In the long-term time frame, the methodology needs to incorporate system development decisions (network/generation expansion plan) as well as asset management planning (usually planned a year ahead). Both are known by the TSO and are easy to accommodate in our methodology. Next, the methodology could be extended to account for possible updates in the approach to $(N-1)$ security (e.g., deterministic vs risk-based criterion [36], [38]), including RES stochasticity and new types of control means available to the TSO such as electricity storage or flexibility from distribution systems upon coordination with distribution system operators [38]).

Once more refined data and information about the above factors are available, they can be used to further improve the realism of the results produced by the proposed generic methodology, which will be applied repeatedly and with updated data for smaller time horizons (e.g., 5 years ahead), assisting the TSOs during each time period of the energy transition.

IV. Conclusions and Future Work

The paper has explored the under-addressed topic of RPRs scarcity through the energy transition toward a renewable-dominated energy supply. To this end, the paper has proposed a novel, comprehensive, and realistic methodology to identify when the issue of RPRs scarcity during plausible scenarios of the energy transition would become severe. The computational core of the proposed methodology comprises four different AC security-constrained optimal power flow (SCOPF) problems: one conventional, two tailored ones that assess the RPRs scarcity in production and absorption modes, respectively, and an optimal reactive power dispatch. As these problems are non-convex, local optimizers like IPOPT can theoretically guarantee only a local optimum. However, since extensive empirical evidence in the power systems area shows in practice that the solution provided by local optimizers is also the global optimum in most generic AC OPF problem instances [39], there are good chances that the solution of AC SCOPF problems is the global optimum.

The methodology is versatile, offering the possibility to assess RPRs in different time scales, ranging from day-ahead short-term operation to years-ahead long-term operation while considering appropriate renewable energy production forecasts and day-dependent load profiles.

The proposed methodology can serve as a decision-making support tool for the TSOs, allowing them to plug and play distinct plausible energy transition scenarios (e.g., differing in terms of sequence and timing of: phased out of power plants as well as location, type, and size of renewable energy sources deployed). Although inspired by the European countries' decarbonization process, where the energy transition scenarios focus typically on replacing fossil fuel generation with mostly wind and solar RES, the methodology is generic and can be applied with minor adaptations to any other specific context, including different combinations (types and mix) of electricity production sources (e.g., hydro, nuclear, biomass).

The value of the proposed methodology has been extensively demonstrated in the 60-bus Nordic32 system while its tractability has been empirically proved in a large 1,203-bus system.

The numerical results have shown that: (i) due to the complex interactions in energy transition scenarios, in some cases, the RPRs behaviour in time is counter-intuitive and thereby cannot be predicted with simpler techniques, supporting the proposed methodology, (ii) the capability of generators to absorb reactive power at light load is often more constraining than their capability to produce reactive power at peak load, and (iii) optimizing power system operation based on the conventional SCOPF reinforces generally the amount of RPRs and delays considerably the time when they become scarce.

The methodology sheds light on some hurdles in the ongoing energy transition and informs the TSO about the timing where RPRs become insufficient to maintain security. Accordingly, our future work will address the var planning problem, i.e., optimal placement of static or dynamic sources of RPRs, to strengthen the grid and face RPRs scarcity.

Acknowledgement

The authors thank Dr. Muhammad Usman and Dr. Mohammad Iman Alizadeh, both from LIST, for valuable support with coding aspects of the methodology and Dr. Efthymois Karangelos (ULg) for constructive remarks on the methodology.

References

[1] European Commission, "A European Green Deal," [Online]. Available: https://ec.europa.eu/info/strategy/priorities-2019-2024/european-green-deal_en.

[2] K. Hainsch, K. Löffler, T. Burandt, H. Auer, P. C. del Granado, P. Pisciella, and S. Zwickl-Bernhard, "Energy transition scenarios: What policies, societal attitudes, and technology developments will realize the EU Green Deal?," *Energy*, p. 122067, 2021.

[3] MIGRATE, "Massive InteGRATion of power Electronic devices – Current and arising issues caused by increasing power electronics penetration," [Online; accessed: 15-Dec-2016]. Available: https://ec.europa.eu/research/participants/documents/downloadPublic?documentIds=080166e5af08ecd7&appId=PPGMS.

[4] F. Capitanescu, "Evaluating reactive power reserves scarcity during the energy transition toward 100% renewable supply," *Electric Power Systems Research*, vol. 190, p. 106672, 2021.

[5] T. K. Vrana, D. Flynn, E. Gomez-Lazaro, J. Kiviluoma, D. Marcel, N. Cutululis, and J. C. Smith, "Wind power within European grid codes: Evolution, status and outlook," *Wiley Interdisciplinary Reviews: Energy and Environment*, vol. 7, no. 3, pp. 1–21, 2018.

[6] C. MacIver, K. Bell, and M. Nedd, "An analysis of the August 9th 2019 GB transmission system frequency incident," *Electric Power Systems Research*, vol. 199, p. 107444, 2021.

[7] IEEE Std 1547–2018, "IEEE standard for interconnection and interoperability of distributed energy resources with associated electric power systems interfaces," *Sponsored by the IEEE Standards Coordinating Committee 21 on Fuel Cells, Photovoltaics, Dispersed Generation, and Energy Storage*, Approved 15 February 2018.

[8] International Renewable Energy Agency (IRENA), Abu Dhabi, "Grid Codes for Renewable Powered Systems," 2022. [Online]. Available: https://www.irena.org/publications/2022/Apr/Grid-codes-for-renewable-powered-systems.

[9] E. Vaahedi, Y. Mansour, C. Fuchs, S. Granville, M. D. L. Latore, and H. Hamadanizadeh, "Dynamic security constrained optimal power flow/VAr planning," *IEEE Transactions on Power Systems*, vol. 16, no. 1, pp. 38–43, 2001.

[10] R. A. Jabr, N. Martins, B. C. Pal, and S. Karaki, "Contingency Constrained VAr Planning Using Penalty Successive Conic Programming," *IEEE Transactions on Power Systems*, vol. 27, no. 1, pp. 545–553, 2011.

[11] W. Xu, Y. Zhang, L. C. da Silva, P. Kundur, and A. A. Warrack, "Valuation of dynamic reactive power support services for transmission access," *IEEE Transactions on Power Systems*, vol. 16, no. 4, pp. 719–728, 2001.

[12] K. Bhattacharya and J. Zhong, "Reactive power as an ancillary service," *IEEE Transactions on Power Systems*, vol. 16, no. 2, pp. 294–300, 2001.

[13] P. Frias, T. Gomez, and D. Soler, "A Reactive Power Capacity Market Using Annual Auctions," *IEEE Transactions on Power Systems*, vol. 23, no. 3, pp. 1458–1468, 2008.

[14] K. L. Anaya and M. G. Pollitt, "Reactive power procurement: A review of current trends," *Applied Energy*, vol. 270, p. 114939, 2020.

[15] P. A. Ruiz and P. W. Sauer, "Reactive power reserve issues," in *2006 38th North American Power Symposium*, pp. 439–445, 2006.

[16] O. A. Mousavi and R. Cherkaoui, "Literature Survey on Fundamental Issues of Voltage and Reactive Power Control." École Polytechnique Fédérale de Lausanne: Lausanne, Switzerland, 2011.

[17] F. Capitanescu and T. Van Cutsem, "Evaluation of reactive power reserves with respect to contingencies," in *Proc. International Workshop on Bulk Power System Dynamics and Control V*, pp. 310–318, 2001.

[18] Y. Choi, S. Seo, S. Kang, and B. Lee, "Justification of Effective Reactive Power Reserves With Respect to a Particular Bus Using Linear Sensitivity," *IEEE Transactions on Power Systems*, vol. 26, no. 4, pp. 2118–2124, 2011.

[19] H. Song, B. Lee, S.-H. Kwon, and V. Ajjarapu, "Reactive reserve-based contingency constrained optimal power flow (RCCOPF) for enhancement of voltage stability margins," *IEEE Transactions on Power Systems*, vol. 18, no. 4, pp. 1538–1546, 2003.

[20] F. Capitanescu, "Assessing Reactive Power Reserves With Respect to Operating Constraints and Voltage Stability," *IEEE Transactions on Power Systems*, vol. 26, no. 4, pp. 2224–2234, 2011.

[21] K. Zhang, G. Geng, and Q. Jiang, "Online Tracking of Reactive Power Reserve For Wind Farms," *IEEE Transactions on Sustainable Energy*, vol. 11, no. 2, pp. 1100–1102, 2019.

[22] K. C. Sharma, P. Jain, and R. Bhakar, "Wind Power Scenario Generation and Reduction in Stochastic Programming Framework," *Electric Power Components and Systems*, vol. 41, no. 3, pp. 271–285, 2013.

[23] B. Singh and D. Pozo, "A guide to solar power forecasting using ARMA models," in *2019 IEEE PES Innovative Smart Grid Technologies Europe (ISGT-Europe)*, pp. 1–4, IEEE, 2019.

[24] A. Monticelli, M. Pereira, and S. Granville, "Security-constrained optimal power flow with post-contingency corrective rescheduling," *IEEE Transactions on Power Systems*, vol. 2, no. 1, pp. 175–180, 1987.

[25] I. El-Samahy, K. Bhattacharya, C. Canizares, M. F. Anjos, and J. Pan, "A Procurement Market Model for Reactive Power Services Considering System Security," *IEEE Transactions on Power Systems*, vol. 23, no. 1, pp. 137–149, 2008.

[26] Elia, "Study on the future design of the ancillary service of voltage and reactive power control," [Online; accessed: 31-Oct-2018]. Available: https://www.elia.be/en/search#s13_e=0&s13_q=ancillary%20service.

[27] National Grid ESO, "Future of Reactive Power Project Market Design – Project Conclusions," [Online; accessed: Apr-2022]. Available: https://www.nationalgrideso.com/balancing-services/reactive-power-services/reactive-reform-market-design.

[28] I. Aravena, D. K. Molzahn, S. Zhang, C. G. Petra, F. E. Curtis, S. Tu, A. Wächter, E. Wei, E. Wong, A. Gholami, *et al.*, "Recent Developments in Security-Constrained AC Optimal Power Flow: Overview of Challenge 1 in the ARPA-E Grid Optimization Competition," *arXiv preprint arXiv:2206.07843*, 2022.

[29] W. Rosehart, C. Roman, and A. Schellenberg, "Optimal power flow with complementarity constraints," *IEEE Transactions on Power Systems*, vol. 20, no. 2, pp. 813–822, 2005.

[30] F. Capitanescu, W. Rosehart, and L. Wehenkel, "Optimal power flow computations with constraints limiting the number of control actions," *IEEE PES PowerTech, Bucharest, Romania*, pp. 1–8, 2009.

[31] "Nordic32 system," [Online]. Available: https://github.com/MATPOWER/matpower/blob/master/data/case60nordic.m.

[32] I. Dunning, J. Huchette, and M. Lubin, "JuMP: A modeling language for mathematical optimization," *SIAM review*, vol. 59, pp. 295–320, 2017.

[33] A. Wächter, L. Biegler, Y. Lang, and A. Raghunathan, "IPOPT: An interior point algorithm for large-scale nonlinear optimization," [Online]. Available: https://github.com/coin-or/Ipopt.

[34] SINTEF Energy Research, "Energy efficiency and load curve impacts of commercial development in competitive markets-phase 1 – basis for demand response," [Online; accessed 11-Dec-2003]. Available: https://www.sintef.no/globalassets/project/efflocom/efflocom-report-no.-1-basis-for-load-management1.pdf.

[35] Y. Fu, M. Shahidehpour, and Z. Li, "Security-constrained unit commitment with AC constraints," *IEEE Transactions on Power Systems*, vol. 20, no. 2, pp. 1001–1013, 2005.

[36] Q. Wang, J. D. McCalley, T. Zheng, and E. Litvinov, "A Computational Strategy to Solve Preventive Risk-Based Security-Constrained OPF," *IEEE Transactions on Power Systems*, vol. 28, no. 2, pp. 1666–1675, 2012.

[37] Y. Liu, M. C. Ferris, and F. Zhao, "Computational Study of Security Constrained Economic Dispatch With Multi-Stage Rescheduling," *IEEE Transactions on Power Systems*, vol. 30, no. 2, pp. 920–929, 2014.

[38] M. I. Alizadeh, M. Usman, and F. Capitanescu, "Envisioning security control in renewable dominated power systems through stochastic multi-period ac security constrained optimal power flow," *International Journal of Electrical Power & Energy Systems*, vol. 139, p. 107992, 2022.

[39] C. Coffrin, H. L. Hijazi, and P. Van Hentenryck, "The QC Relaxation: A Theoretical and Computational Study on Optimal Power Flow," *IEEE Transactions on Power Systems*, vol. 31, no. 4, pp. 3008–3018, 2015.

Elnaz Davoodi received the master and Ph.D. degrees in the Electrical Power engineering from the University of Tabriz, Tabriz, Iran, in 2012 and 2018, respectively. Her main areas of research interest are modeling and analysis of energy systems particularly in the planning and operation of transmission systems through optimization techniques and optimal power flow approaches.

Florin Capitanescu (Member, IEEE) received the Electrical Power Engineering degree from the Politehnica University of Bucharest, Bucharest, Romania, in 1997, and the Ph.D. degree from the University of Liège, Liège, Belgium, in 2003. Since 2015, he has been a senior researcher with the Luxembourg Institute of Science and Technology, Esch-sur-Alzette, Luxembourg. His main research interests include the application of optimization methods to the operation of transmission and active distribution systems, particularly optimal power flow approaches, power systems security, voltage instability, and smart sustainable buildings.

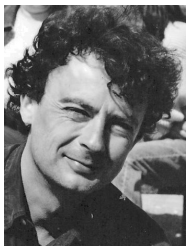

Louis Wehenkel graduated in Electrical Engineering (Electronics) in 1986 and received the Ph.D. degree in 1990, both from the University of Liege (Belgium), where he is full Professor of Electrical Engineering and Computer Science. His research interests lie in the fields of stochastic methods for modeling, optimization, machine learning and data mining, with applications in complex systems, in particular large scale power systems planning, operation and control, industrial process control, bioinformatics and computer vision.